



Proposed satellite position determination systems and techniques for Geostationary Synthetic Aperture Radar

Roger M. Fuster*, Marc Fernández Usón, David Casado Blanco
and Antoni Broquetas Ibars

Remote Sensing Lab, Department of Signal Theory and Communications,
Universitat Politècnica de Catalunya, Campus Nord UPC, Edif. D3, 08034, Barcelona, Spain

*Corresponding author, e-mail address: r.martin.fuster@gmail.com

Abstract

This paper proposes two different calibration techniques for Geostationary Synthetic Aperture Radar (GEOSAR) missions requiring a high precision positioning, based on Active Radar Calibrators and Ground Based Interferometry. The research is enclosed in the preparation studies of a future GEOSAR mission providing continuous monitoring at continental scale.

Keywords: Geostationary SAR, Active Radar Calibrator, interferometer.

Introduction

Geostationary Synthetic Aperture Radar (GEOSAR) missions are currently being studied in order to provide continuous monitoring of the Earth on a continental scale [Tomiyasu and Pacelli, 1983]. Multiple applications such as land stability control, natural risks prevention or accurate numerical weather prediction models from water vapour atmospheric mapping would substantially benefit from permanent monitoring given their fast evolution, not observable with present Low Earth Orbit based systems [Wadge et al., 2014].

GEOSAR missions are based on operating a radar payload hosted by a communication satellite in a geostationary orbit. Due to orbital perturbations, the satellite does not follow a perfectly circular orbit, but has a slight eccentricity and inclination that can be used to form the Synthetic Aperture required to obtain images [Ruiz Rodon et al., 2014a].

Two possible bands are presently considered: the L-band to offer continental coverage (~3000 km) with coarse 1 km resolution, and the X-band to achieve higher (10 m) resolution by covering smaller areas (~500 km).

To cope with the large radar propagation loss of GEOSAR operation, a long integration time (up to hours) [Recchia et al., 2016], and an along-track oversampling with a PRF well above the Doppler bandwidth will be considered. In this way, the GEOSAR system can operate with antenna sizes and transmitted powers similar to current LEOSAR missions.

Several sources affect the along-track phase history in GEOSAR missions causing unwanted fluctuations which may result in image defocusing. The main expected

contributors to azimuth phase noise are orbit determination errors, radar carrier frequency drifts, the Atmospheric Phase Screen (APS), and satellite attitude instabilities and structural vibration. In order to obtain an accurate image of the scene after SAR processing, the range history of every point of the scene must be known. This fact requires a high precision orbit modelling and the use of suitable techniques for atmospheric phase screen compensation [Ruiz Rodon et al., 2013]. The other influencing factors like oscillator drift and attitude instability, vibration, etc., must be controlled or compensated.

The exposed orbital determination requirements for this mission (with precisions in the order of magnitude of λ) are well beyond the usual orbit modelling requirements to manage repositioning of satellites in GEO orbits. Two possible precise measurements suitable for accurate orbit determination are discussed in this document. First, a group of Active Radar Calibrators (ARCs) will be explained, and an alternative or complementary technique using a ground based interferometer system will be proposed.

The final goal of both systems is to provide raw positioning data, in such a manner that it can be then processed through different orbital determination techniques, based for example on least-squares method [Montenbruck et al., 2000] providing highly precise orbital parameters.

Proposed tracking based on ARC

The usage of an Active Radar Calibrator in GEOSAR is proposed to provide accurate delay (range) and phase (Doppler) measurements for precise orbit tracking (Fig. 1). In this way, the range history of every point of the observed scene can be predicted in the azimuth compression step of the SAR processor.

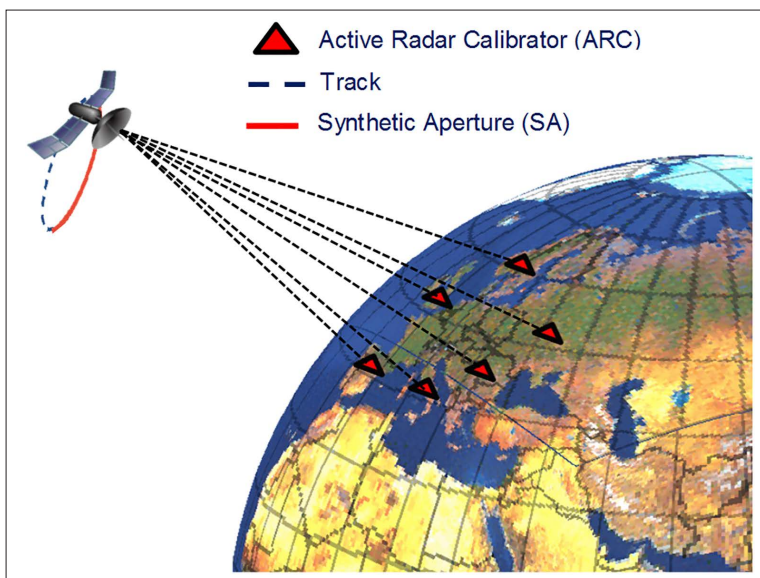


Figure 1 - Basic geometry of the ARC system, featuring several active reflectors spread across Europe and the GEOSAR satellite. Not on scale.

In contrast to ad-hoc orbit determination systems like GNSS for GEO, DORIS, PRARE [Montenbruck et al., 2000], etc., the ARC based SAR tracking has three advantages:

The Range observables provided by the ARC are coincident to those required in SAR processing: Range history. This minimizes possible Dilution of Precision issues induced by poor measurement geometry in a complementary positioning system;

ARC provides phase data at the SAR operation carrier which minimizes atmospheric channel errors and allows similar level of phase precision with respect to SAR processing requirements; The Range and Phase measurements correspond to the SAR antenna phase centre, avoiding uncertainties and errors related to lever-arm vectors between different satellite radar and navigation subsystems and subsequent requirements on attitude concurrent measurement and control, etc.

Moreover, as corner reflectors in LEOSAR, amplitude and phase stable ARC of well-known Radar Cross Section (RCS) and accurately located on the Earth surface can be used for image Radiometric/Geometric calibration. In addition, the ARC observation is able to provide valuable data for Atmospheric Phase Screen modelling and compensation [Recchia et al., 2014].

To accomplish these objectives, both X-band and L-band operation frequencies have been considered in the preliminary design of a GEOSAR ARC. The ARC consists basically on a receiving antenna with gain G_{rc} followed by a linear amplifier with gain G_{ac} and a transmitter antenna with gain G_{tc} . The resulting RCS is

$$\sigma \text{ (dBsm)} = G_{rc} \text{ (dB)} + G_{ac} \text{ (dB)} + G_{tc} \text{ (dB)} + 20 \log(\lambda) - 10 \log(4\pi) - L \text{ (dB)} \quad [1]$$

where L accounts for cabling losses. In the design, the gain of both antennas have been considered equal, $G_{rc} = G_{tc}$. Assuming the antenna is a parabolic reflector, its gain can be expressed as a function of the reflector's diameter D , the illumination efficiency η and losses L_a .

$$G_{ant} = (\pi D / \lambda)^2 \eta L_a \quad [2]$$

Pyramidal sub-aperture processing with phase compensation

The ARC to be used for orbit determination should provide time delay and phase measurements in a pulse to pulse basis to avoid phase ambiguities in calibrators close to the antenna spot limits. This is strictly true for radars operating with Pulse Repetition Frequency (PRF) equal to the Nyquist limit related to the SAR Doppler bandwidth. In the case of GEOSAR, due to the slow radar-scene motion and transmitter technological reasons, the PRF is expected to be well above the SAR Doppler bandwidth. This will allow using 'pre-summing', a coherent integration of pulses during the echo correlation time, to increase the signal SNR before range and Doppler measurements. Therefore, in the ARC design, an optimum integration time for calibration must be computed in agreement to the SAR operation parameters. In our analysis, we will consider an initial integration time equal to the inverse of the Doppler bandwidth which is below 3 Hz both for X and L considered bands.

In addition to the phase and amplitude stability and TX-RX isolation, designing an ARC for GEOSAR calibration is specially challenging due to the large radar-Earth range and high clutter levels associated with the large antenna foot-print [Ruiz Rodon et al., 2014b]. Brute force design providing both large Signal to Noise (SNR) and Signal to Clutter (SCR) ratios

results in very large reflectors and high gain amplifiers, increasing cost and compromising the design stability.

It is interesting to remark that a coherent extension of the integration time of ARC echoes beyond their Doppler bandwidth correlation time would proportionally increase both SNR and SCR. This would be only possible if the phase history of the ARC signal induced by the satellite motion could be compensated. This phase-compensated coherent integration is simply a Synthetic Aperture Formation resulting in the azimuth resolution cell reduction, which is the reason of the commented SCR improvement. However, the phase-history compensation of the ARC cannot be performed without knowing precisely the satellite orbit. This difficulty can be circumvented proceeding in a stepped way, by forming a pyramid of sub-apertures [Ruiz Rodon et al., 2013].

Based on short-term high correlation of orbital parameters, an approximate orbit model will allow to extend significantly the Doppler based integration time by forming a small coherent sub-aperture. In this way, both SNR and SCR can be increased sufficiently in order to provide useful range and Doppler ARC measurements. From the ARC measurements the initial orbit parameters can be improved enough to extend the capability of coherent integration of ARC echoes along a larger upper level sub-aperture. The longer integration time will provide a better SNR/SCR and a better orbital estimation. Although for clarity we are referring to a single ARC, increasing the number of observed calibrators will provide a better orbit determination and better rejection of atmospheric artefacts, which may distort the range and phase measurements.

The orbit improvements could be used both to reprocess the initial small sub-aperture with better motion compensation and to extend even more the integration time providing higher quality observations. The procedure will stop once the final aperture is formed. Please note that the number of sub-apertures in every step will decrease as the sub-aperture length increases, which can be summarized in the pyramid of Figure 2. It must be taken into account that in all sub-apertures the range dimension of the resolution cell is the same, according to the transmitted pulse bandwidth. However, the azimuth cell size will decrease when processing upper levels of the pyramid, while SAR processing gain of point scatterers will increase in the same factor. This fact is very relevant for APS compensation during calibration, since the stronger scattering points of the scene, undetectable in raw data, are expected to be visible becoming potential calibrators of opportunity at intermediate and higher levels of the pyramid, increasing the density of calibration network in this way. The APS is expected to affect predominantly the higher levels of the pyramid due to the intrinsic spatial and temporal correlation of the atmosphere.

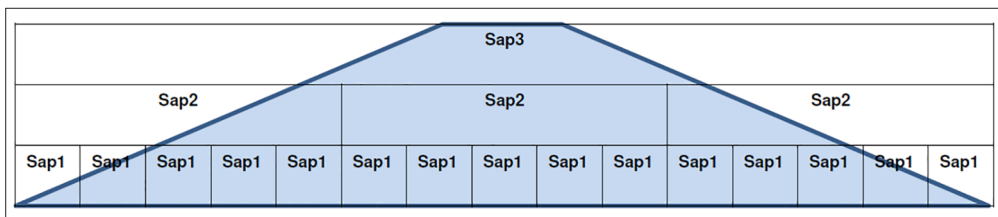


Figure 2 - Three level sub-aperture processing scheme. The bottom level features a larger number of processed blocks with shorter apertures. As we ascend into the scheme, the processed blocks are reduced and the aperture size is increased until we reach the full aperture processing.

L-band ARC parameters

Both X- and L-band preliminary ARC designs have been completed using 1 m diameter reflectors and moderate amplifier gains as shown in Table 1 for the case of L-band. In the case of X-band, the reflector size and required amplifier gains are smaller. The required power outputs are in the order of few dBm in both bands. Table 2 shows the achieved SNR and SCR with the proposed L-band ARC for the pre-summing case and different proposed sub-apertures. The possibility of phase coding the ARC signal path has been studied to increase SCR and to allow surface and ARC signal separation during SAR processing.

Table 1 - Design parameters of the L-band ARC.

L-ARC	Unit	
RX Antenna Diam.	m	1
Antenna efficiency		0.75
Antenna losses	dB	1
Antenna Gain	dB	20.2
TX Antenna Diam.	m	1
Antenna efficiency		0.75
Antenna losses	dB	1
Antenna Gain	dB	20.2
Amplifier Gain	dB	45
Cabling Longitude	m	4
Cabling Losses	dB	5.3
ARC RCS	dBsm	62.6
Amplitude Isolation Req.	dB	83.4
Phase Isolation Req.	dB	66.2

Table 2 - SNR and SCR obtained with L-band ARC.

L-ARC SNCR	Unit				
Sub-aperture		Pre-sum 1/Bd	SA1	SA2	SA3
Integration time	s	0.763	16	480	14400
SA Length	m	3.755	78.7	2360.9	70827.2
SNR	dB	24.8	38	52.8	67.53
unicoded ARC SCR					
azimuth resolution	m	1200837	57292	1909.7	63.6
range resolution	m	50.4			
SCR uncoded	dB	5.9	19.11	33.9	48.65
coded ARC SCR					
Clutter rejection	dB	20	20	20	20
SRC coded	dB	25.9	39.11	53.9	68.65

A phase/amplitude compensated Active Radar Calibrator

To achieve stable RCS and phase delay a balanced configuration is proposed (Fig. 3). Instead of designing a costly highly stable signal path, the amplitude and phase of the ARC is maintained constant by a reference passive cable, which is inherently more stable and easier to maintain at a constant temperature. Calibration pulses are routed through both the reference stable cable and ARC main path allowing compensating ARC amplitude and phase drifts by balancing both errors using a variable attenuator and a phase shifter. Note that in the proposed design the antenna feeders are included in the calibration loop.

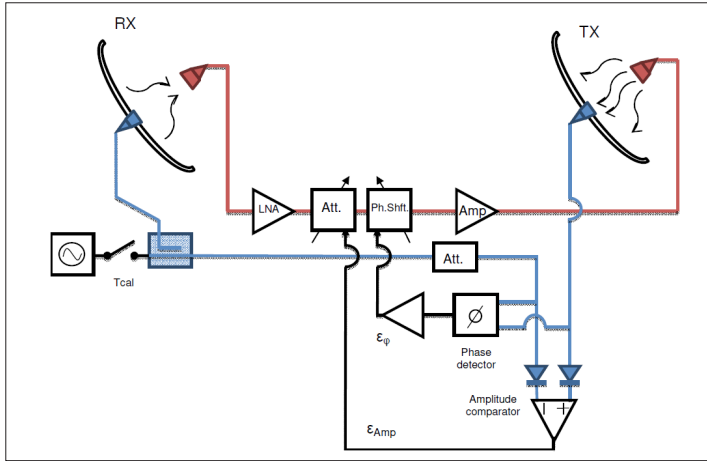


Figure 3 - Schematic of the ARC loop implementation to provide phase and amplitude compensation caused by atmospheric fluctuations.

Proposed tracking using ground based interferometry

Some decades have passed since the beginning of interferometry and its applications have reached several fields such as radio astronomy, metrology, quantum mechanics or remote sensing. Interferometry techniques are based on the measurement of phase difference between receivers, which is related with the position of both the transmitter and the receivers. This section covers the fundamentals of a ground based interferometer aimed to serve as high precision observable for geostationary orbit positioning.

Interferometric phase retrieving

The basic ground based interferometer configuration is formed by 3 elements: the transmitting satellite and two accurately located ground receivers. The arriving signals at each receiving antenna will be the same complex signal with slightly different delay resulting in a phase difference component.

$$Tx(t) = |Tx(t)| e^{j\angle Tx(t)} \quad [3]$$

$$Rx_i(t) = |Tx(t)| e^{j\angle Tx(t)} e^{ja_i(t)} \quad [4]$$

Where $T_x(t)$ is the complex transmitted signal expressed in polar notation whereas R_i and a_i are the received signal and its arrival phase at receiver. By executing a lag zero, limited time, discrete complex cross-correlation processing, the interferometric phase can be obtained.

$$R_{(R_{X_1}, R_{X_2})}(0) = \frac{1}{T} \sum_0^{kT} R_{X_1}^*(n) R_{X_2}(n) = E_T e^{-j(a_1 - a_2)} \quad [5]$$

Where E_T is the transmitted signal energy, T is the time period, and k is the sampling ratio. This equation is valid as long as kT is significantly larger than the bandwidth inverse and small enough to consider the phase difference as a constant in that time period. This equation will only deliver data every T seconds, and therefore this will be the time resolution of the system as long as real-time data is needed.

Geometrical model and position tracking

Once the interferometric phase is retrieved, a geometrical model is needed to relate the interferometric phase with a set of position parameters. First, a coordinates system is defined using the Earth as a static reference, as shown in Figure 4. Using this coordinate frame, a phase-position relationship can be defined by expressing the interferometric phase in terms of a time delay. Then, the delay can be translated to an Euclidean distance dependency. This formula is presented in both Cartesian and spherical coordinates:

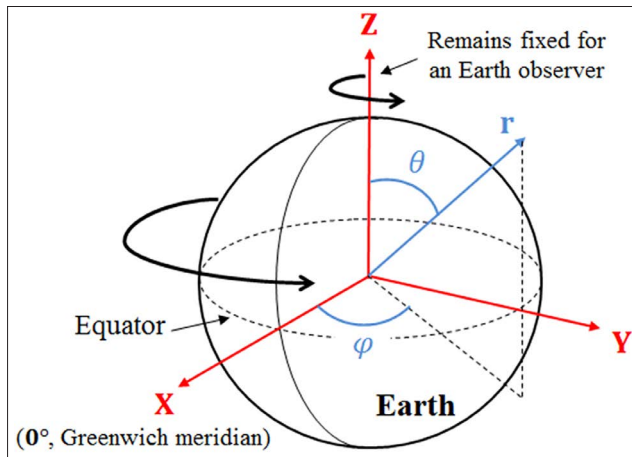


Figure 4 - Geometrical coordinate framework for the interferometer system defined as Earth Centered, Earth Fixed.

$$\Delta a_{i,j} = K \left(\sqrt{(x_i - x_s)^2 + (y_i - y_s)^2 + (z_i - z_s)^2} - \sqrt{(x_j - x_s)^2 + (y_j - y_s)^2 + (z_j - z_s)^2} \right) \quad [6]$$

$$\Delta a_{i,j} = K \left(\sqrt{r_i^2 + r_s^2 - 2r_i r_s \left(\sin(\theta_i) \sin(\theta_s) \cos(\phi_i - \phi_s) + \cos(\theta_i) \cos(\theta_s) \right)} \right. \\ \left. - \sqrt{r_j^2 + r_s^2 - 2r_j r_s \left(\sin(\theta_j) \sin(\theta_s) \cos(\phi_j - \phi_s) + \cos(\theta_j) \cos(\theta_s) \right)} \right) \quad [7]$$

Following the logic of a classic interferometer [Thompson et al., 1986], the accuracy of the system will be determined by the baselines defined between receivers. Although the satellite-receiver range is present in Equation [7], the interferometer fundamentally retrieves angular data, which directly affects the detected interferometric phase. Equations [6] and [7] have a non-algebraical solution for the position parameters. For this reason, numerical methods must be applied in order to obtain the position vector.

Proposed implementation

One of the main advantages of this technique is the capability to be tested and verified with actual geostationary communication satellite systems. The opportunity signal chosen for this first implementation is a TV broadcast from ASTRA 1M satellite located at the 19.2° E slot.

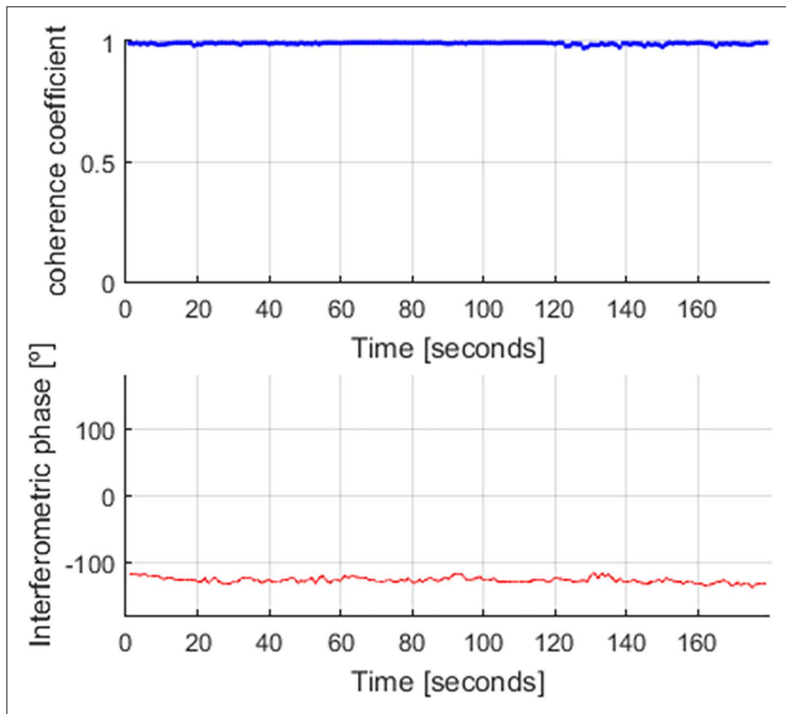


Figure 5 - End-to-end validation test, depicting the coherence coefficient and interferometric phase detected by the system when using a fixed locally emitted source.

A low resolution scheme is under development and it is expected to retrieve results during the year 2016. The current state of the project features two close-by receivers receiving signal in a coherent manner by synchronising two standard universal LNB receivers by means of a reference signal.

This signal is the down-converted from the intermediate frequency on a coherent demodulator and digitized to process the zero lag correlation by software. An end-to-end experiment has been successfully completed retrieving data from a laboratory generated emission on a still antenna using a relatively short integration time of 1 s. As shown in the resulting Figure 5, the correlation factor is close to the unity, which indicates high correlation between signals, and the interferometric phase is constant in time with an added noise component.

Conclusions

The ARC system provides high range accuracy on each observation, creating an accurate range history of the satellite. This system consist on a minimum of three ARC placed at the border of the illuminated area, improving its resolution and functionality using redundancy adding more ARCs on the scene.

With the proposed ARC antenna sizes and amplifier gains, several calibrators can be deployed and operated at moderate cost providing excellent scattering point references with high RCS for GEOSAR precise satellite ranging. On the other hand, the interferometric approach is able to provide high precision angular data. Both systems can be used for satellite continuous monitoring providing the observables required for precise orbital determination techniques.

Since the interferometer is fundamentally a passive system, it can be properly implemented, tested and validated by using an opportunity signal before the actual GEOSAR satellite is launched. The short baseline proposed in this paper is the starting point of a research that will eventually lead to a VLBI (Very Large Baseline Interferometer) configuration [Sasao and Fletcher, 2010], expected to retrieve unprecedented accuracy on satellite tracking.

The proposed systems are not mutually exclusive by definition and a multi instrument tracking system could be implemented using both of them. Future studies will address the processing of the positioning data in order to obtain an accurate orbital model and validate experimentally the proposed techniques.

Acknowledgements

This work has been financed by the Spanish Science, Research and Innovation Plan (MINECO) with Project Code TIN2014-55413-C2-1-P.

References

- Montenbruck O., Gill, E. (2000) - *Satellite Orbits: Models, Methods, and Applications*. Springer. doi: <http://dx.doi.org/10.1007/978-3-642-58351-3>.
- Recchia A., Guarnieri A.M., Broquetas A., Leanza A. (2016) - *Impact of Scene Decorrelation on Geosynchronous SAR Data Focusing*. IEEE Transactions on Geoscience and Remote Sensing, 54 (3): 1635-1646. doi: <http://dx.doi.org/10.1109/TGRS.2015.2486385>.
- Recchia A., Monti Guarnieri A., Broquetas A., Ruiz-Rodon J. (2014) - *Assessment of atmospheric phase screen impact on Geosynchronous SAR*. IEEE International

- Symposium on Geoscience and Remote Sensing (IGARSS), pp. 2253-2256, 13-18 July.
- Ruiz Rodon J., Broquetas A., Monti Guarnieri A., Rocca F. (2013) - *Geosynchronous SAR Focusing With Atmospheric Phase Screen Retrieval and Compensation*. IEEE Transactions on Geoscience and Remote Sensing, 51 (8): 4397-4404. doi: <http://dx.doi.org/10.1109/TGRS.2013.2242202>.
- Ruiz Rodon J., Broquetas A., Makhoul E., Monti Guarnieri A., Rocca F. (2014a) - *Nearly Zero Inclination Geosynchronous SAR Mission Analysis With Long Integration Time for Earth Observation*. IEEE Transactions on Geoscience and Remote Sensing, 52 (10): 6379-6391. doi: <http://dx.doi.org/10.1109/TGRS.2013.2296357>.
- Ruiz Rodon J., Broquetas A., Monti-Guarnieri A., Recchia A. (2014b) - *Bistatic Geosynchronous SAR for land and atmosphere continuous observation*. Proceedings of EUSAR 2014, 10th European Conference on Synthetic Aperture Radar, 3-5 June.
- Sasao T., Fletcher A.B. (2010) - *Introduction to VLBI Systems*. Astronomy and Space Science Institute, Seoul, South Korea: Korea.
- Tomiyasu K., and Pacelli J.L. (1983) - *Synthetic Aperture Radar Imaging from an Inclined Geosynchronous Orbit*. IEEE Transactions on Geoscience and Remote Sensing, GE-21 (3): 324-329. doi: <http://dx.doi.org/10.1109/TGRS.1983.350561>.
- Thompson A.R., Moran J.M., Swenson Jr. C.W. (1968) - *Interferometry and Synthesis in Radio Astronomy*. John Wiley & Sons.
- Wadge G., Guarnie A.M., Hobbs S.E., Schul D. (2014) - *Potential atmospheric and terrestrial applications of a geosynchronous radar*. IEEE International Symposium on Geoscience and Remote Sensing (IGARSS), pp. 946-949, Quebec City, QC. doi: <http://dx.doi.org/10.1109/igarss.2014.6946582>.

© 2016 by the authors; licensee Italian Society of Remote Sensing (AIT). This article is an open access article distributed under the terms and conditions of the Creative Commons Attribution license (<http://creativecommons.org/licenses/by/4.0/>).